NEUTRAL HYDROGEN IN THE IRREGULAR GALAXY NGC 3109

By K. J. van Damme*

[*Manuscript received June* 30, 1966]

Summary

The galaxy NGC 3109 was investigated at 21 cm wavelength with the 210 ft radio telescope at Parkes. For a distance $d = 2 \cdot 2$ Mpc the total mass of neutral hydrogen is $M_{\mathrm{H}} = 2 \cdot 2 \times 10^9 \, M_{\odot}$ (corrected for self-absorption). The rotation curve has been determined and, after correction for beamwidth effects, the total mass computed to be $M_{\mathrm{T}} = 0 \cdot 6 \times 10^{10} \, M_{\odot}$. Then $M_{\mathrm{H}}/M_{\mathrm{T}} = 0 \cdot 36$, $M_{\mathrm{H}}/L_{\mathrm{pg}} = 2 \cdot 8$, and $M_{\mathrm{T}}/L_{\mathrm{pg}} = 7 \cdot 5$.

I. Introduction

Previous work on the irregular galaxy NGC 3109 has been carried out by Epstein (1964) with the Harvard 60 ft radio telescope. The present paper describes 21 cm hydrogen line observations made with the 210 ft radio telescope at Parkes (Bowen and Minnett 1962).

The galaxy was completely scanned in declination with a 3 dB beamwidth of $13' \cdot 5$ arc at frequencies covering its whole radial velocity range. Line profiles have been constructed for a grid of 72 points. The rotation curve has been determined, and an attempt has been made to correct its shape for smoothing by the finite beamwidth.

II. Observing Procedure

A double-parametric frequency switching receiver was used (Robinson 1963). With a time constant of 15 sec, a 3 dB bandwidth of 140 kc/s (corresponding to a velocity spread of $30 \cdot 4$ km/sec), and a system noise temperature of about 180°K, r.m.s. fluctuations of about $0 \cdot 35$ degK could be expected in the receiver output. When the input was balanced at signal and reference frequencies the observed fluctuations were close to those anticipated. For a more detailed account of the receiver and its performance, see Robinson and van Damme (1966).

At 1420 Mc/s the 210 ft telescope has a 3 dB beamwidth of $13' \cdot 5$ arc, with nearly circular symmetry and with the near side lobes 20 dB down. The mean beamshape can be closely approximated by the Gaussian function

$$h(r) = \exp(-mr^2), \tag{1}$$

where $m = 0 \cdot 0152$ when r is measured in minutes of arc. The effective solid angle of the beam, Ω'_{B} (Seeger, Westerhout, and van de Hulst 1956), is 207 sq min arc.

From measurements on the discrete source 3C 353, it has been found that the pointing errors lie within $\pm 1'$ arc. The source 3C 353 was also used to calibrate the sensitivity of the antenna–receiver system (Robinson and van Damme 1966). The

* Division of Radiophysics, CSIRO, University Grounds, Chippendale, N.S.W.; present address: 41 Staten Laan, The Hague, The Netherlands.

ratio of the antenna temperature of 3C 353 to a calibration signal from a noise generator was measured frequently. Variations of the ratio between successive observing sessions did not exceed 5%.

Observations were made during the period May 1963 to April 1964, involving about 80 hours of observing time. The galaxy was scanned both ways in declination at intervals of half a beamwidth for successive signal frequencies separated one bandwidth from each other. Scan rates were chosen sufficiently low to avoid amplitude suppression by time constant effects (Howard 1961). A record of average quality is shown in Figure 1. During each observing period, scans through the central regions were repeated to test the consistency of the calibrations.

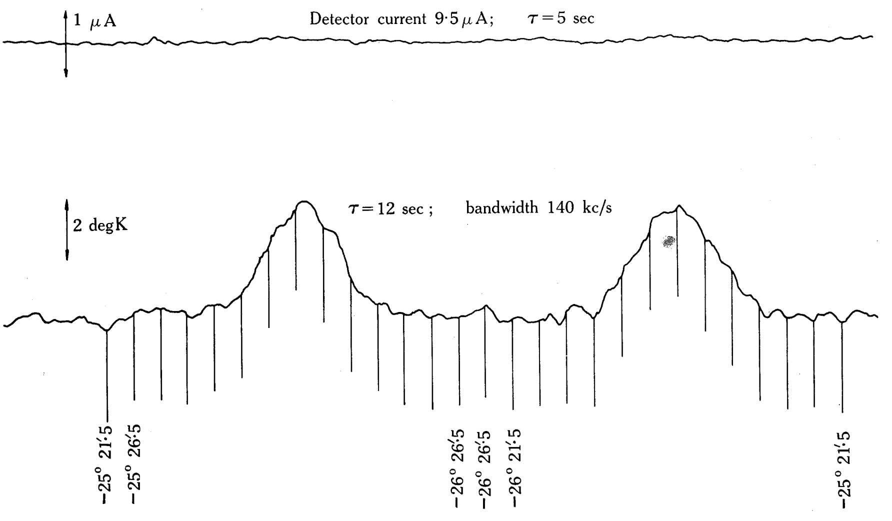

Fig. 1.—Repeated declination scans across NGC 3109 at R.A. $10^{h}01^{m}18^{s}$. Scan rate 0°·15 per minute; radial velocity 410 km/sec.

To define the peaks of the line profiles along the major axis (for the construction of the rotation curve), spot measurements were made using an analogue integrator with an integration time of 100 sec. Reference points were chosen at declination −26° 40′ and at the right ascensions of the corresponding major-axis points.

The reference channel was placed either above or below the signal channel, well clear of radiation from NGC 3109 and the Galaxy. The relative position of the channels did not affect the results.

The detector current (total power output) was recorded continuously as a check on receiver performance and to allow for corrections to the temperature calibration scale based on the known detector law.

III. Optical Characteristics of NGC 3109

The optical charactertistics of NGC 3109 are listed in Table 1. Plate 1 shows a photograph of the galaxy taken with the 20 in. Schmidt camera at Mount Stromlo Observatory, Canberra.

NEUTRAL HYDROGEN IN NGC 3109

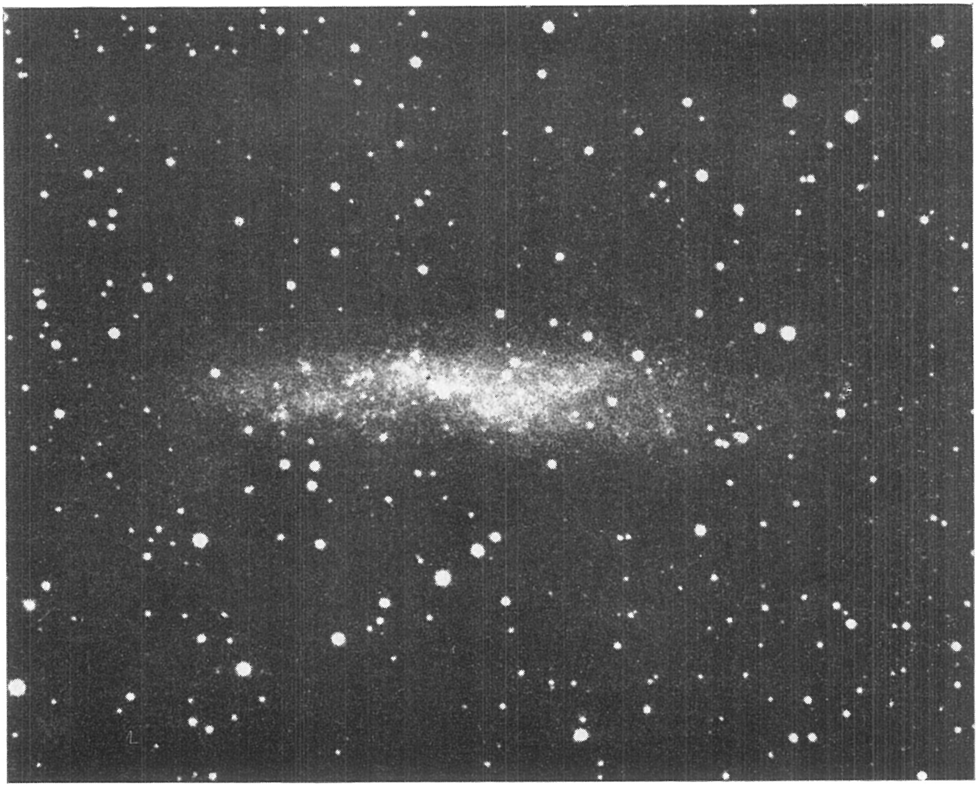

Photograph of NGC 3109 taken with the Uppsala 20–26 in. Schmidt camera at Mount Stromlo Observatory (103aO plate). North is at top, east is to the right. Scale 1 mm = 10″ arc.

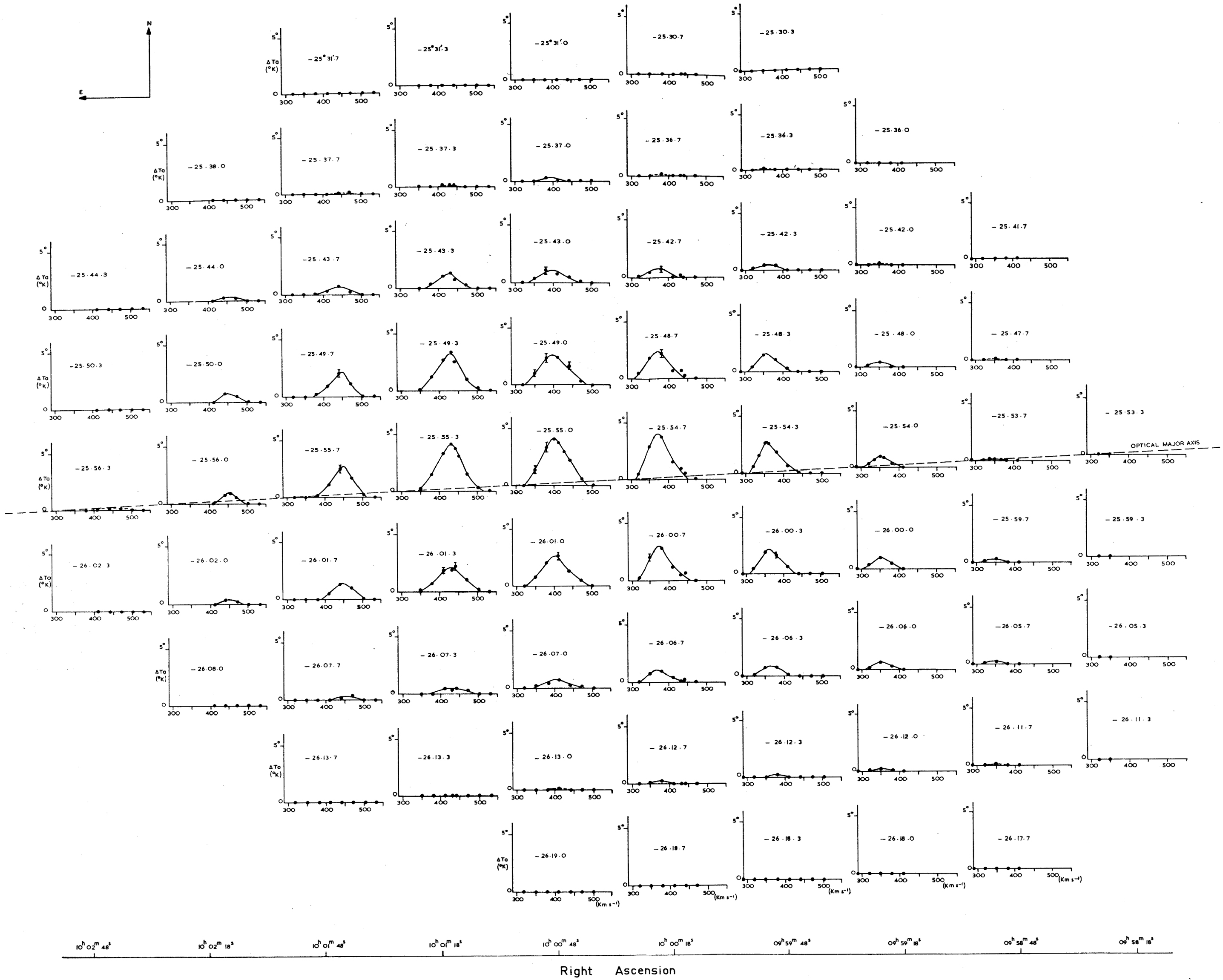

Fig. 2.—Grid of line profiles for NGC 3109. Radial velocities are reduced to the Sun.

The orientation of the major axis, reckoned from west to north, was estimated from three pairs of reference stars chosen from the Palomar Sky Atlas (National Geographic Society 1954–58), the Atlas of the Heavens (Bečkvář 1959), and the General Catalogue (Boss 1963).

TABLE 1

OPTICAL CHARACTERISTICS OF NGC 3109

Type	Irregular
Size*	10′ by 2′ arc
Coordinates (NGC, 1950)	R.A.: $10^{h}\,00^{m}\,48^{s}$ Dec.: $-25°\,55'\cdot 0$
Inclination of principal plane	$i = 90°$ (side on)
Orientation of major axis	$t = 2°\,50'\ (\pm 10')$
Distance†	$d = 2\cdot 2\,c$ Mpc
Luminosity†	$L_{\mathrm{pg}} = 0\cdot 8\,c^2 \times 10^9\,L_{\odot}$
Radial velocity‡	$v_{\mathrm{r}} = +441$ km/sec

* Bečkvář (1959).
† Epstein (1964).
‡ Humason, Mayall, and Sandage (1956).

IV. Reduction of Observations

To plot the line profiles, an oblique coordinate system was constructed with its x axis along the optical major axis and its y axis along the declination circle through the optical centre of the galaxy. The line profiles were derived from the records for a grid of points separated by $6'\cdot 8$ arc along the x axis and by $6'$ arc in declination. Correction was made for the effect of the time constant. Radial velocities were corrected to the Sun. The complete set of profiles is shown in Figure 2. The accuracy of the profile points is better than $\pm 0\cdot 25$ degK, unless otherwise indicated.

V. Mass and Distribution of Neutral Hydrogen

(a) *Hydrogen Mass*

It is well known (van de Hulst, Muller, and Oort 1954; Volders 1959) that the total neutral hydrogen content of a galaxy is given by

$$M_{\mathrm{H}}/M_{\odot} = 3\cdot 10 \times 10^{-6}\,Fc^2d^2 \iiint_{\mathrm{G},\nu} T_{\mathrm{b}}(\theta,\phi,\nu)\,\mathrm{d}\Omega\,\mathrm{d}\nu\,, \tag{2}$$

where T_{b} is the brightness temperature (°K), F is a correction factor for self-absorption, and c is a correction to the distance d (in parsecs). The triple integral is to be taken over the galaxy and its full frequency range, with Ω measured in steradians and ν in cycles per second.

It can easily be shown (see Appendix I) that

$$M_{\mathrm{H}}/M_{\odot} = 3\cdot 10\times 10^{-6}\,Fc^{2}d^{2}\iiint_{\mathrm{D},\nu}\frac{T_{\mathrm{a}}(\theta,\phi,\nu)}{1-\beta}\,\mathrm{d}\Omega\,\mathrm{d}\nu\,, \tag{3}$$

where T_{a} is the antenna temperature produced by the galaxy and β is the antenna stray factor (Seeger, Westerhout, and van de Hulst 1956). The integral is now extended over the convolved source and convolved frequency range.

The mass of neutral hydrogen given by (3) was computed in three ways. Although the last two are not independent of each other, they are useful in judging the accuracy of the reduction procedures.

First, M_{H} was calculated by integrating all declination scans with a planimeter and then integrating over right ascension and frequency. However, the integrations of the repeated scans were not averaged, but the data were processed in such a way that they would lead to a lowest and a highest possible value of M_{H}. The result is

$$1\cdot 55\,c^{2}\times 10^{9} < M_{\mathrm{H}}/F < 1\cdot 89\,c^{2}\times 10^{9}\,M_{\odot}\,. \tag{4}$$

Next, the line profiles (Fig. 2) were integrated by planimeter. Integration over δ and α successively resulted in

$$M_{\mathrm{H}}/F = 1\cdot 76\,c^{2}\times 10^{9}\,M_{\odot}\,. \tag{5}$$

Finally, the integration (3) was performed by constructing the contour map of integrated antenna temperature (Fig. 3). Integration of the contours gave

$$M_{\mathrm{H}}/F = 1\cdot 71\,c^{2}\times 10^{9}\,M_{\odot}\,. \tag{6}$$

The results (5) and (6) are very closely equal to the average value of (4), and they show that the reduction process has not introduced any significant errors. For the total neutral hydrogen mass we shall adopt the value

$$M_{\mathrm{H}}/F = 1\cdot 7\,c^{2}\times 10^{9}\,M_{\odot}\,. \tag{7}$$

(*b*) *Hydrogen Distribution*

On the contour map (Fig. 3) there is a deviation of about 13° between the optical and radio major axes. This could be caused by absorption effects. However, the distribution of luminous material may well be asymmetric about the equatorial plane. A photometric investigation would be required to elucidate this difference. Such an investigation would also yield a better estimate for the optical axis ratio c/a in the oblate spheroid model (Section VI(c)). Moreover, it is useful to convolve the optical isophotes with the antenna beam and to compare the convolved optical galaxy with the HI contour map (Robinson and van Damme 1966).

When corrections for beam broadening have been made (see Appendix II), the size of the radio source is $28\cdot 6\,c \times 12\cdot 8\,c$ kpc. This shows that the hydrogen extends considerably further than the optical dimensions of $6\cdot 4\,c \times 1\cdot 3\,c$ kpc.

The region of maximum HI concentration is slightly displaced from the optical centre, about 3′ arc in increasing right ascension and 1′ arc in positive declination

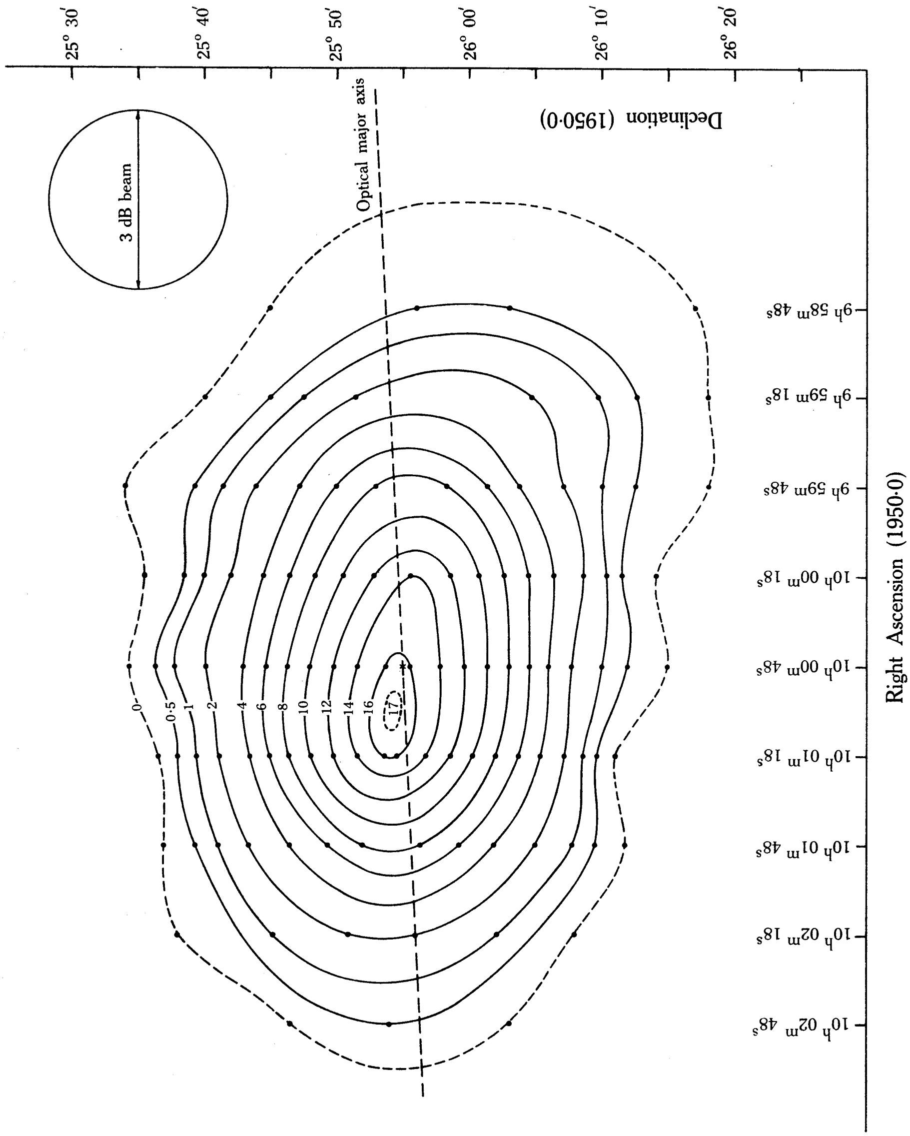

Fig. 3.—Contour map of $\int T_a \, d\nu$. Contour unit is 10^5 degK (c/s). Declination values are negative.

(corresponding to $1 \cdot 9\,c$ kpc and $0 \cdot 6\,c$ kpc respectively). The difference is a little greater than the pointing accuracy of the telescope and could be produced by absorption or by asymmetry of the luminosity distribution (see above). The contour map does not show any structure. It is unlikely that the undulating patterns of the outer contours are significant.

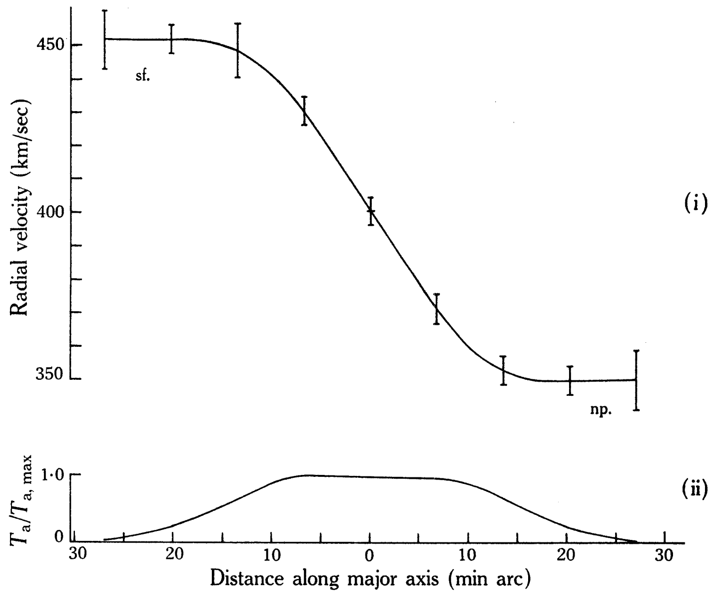

Fig. 4.—(i) Observed rotation curve along the major axis of NGC 3109; (ii) normalized variation of peak profile antenna temperatures along the major axis.

VI. Total Mass

(a) *Observed Rotation Curve*

The observed rotation curve (Fig. 4) of the galaxy was obtained from the line profiles along the major axis (Fig. 2). An attempt has been made to indicate the uncertainties in the velocities at which the profile peaks occur. No correction was applied for inclination of the galaxy, the system being edge-on. The rotation curve is fairly symmetric, and the centre of rotation coincides with the optical centre. For the systemic radial velocity we find $v_r = 401(\pm 5)$ km/sec. This compares well with the value of $403(\pm 10)$ km/sec determined by Epstein (1964). The optical value is 441 km/sec (Humason, Mayall, and Sandage 1956). The 10% difference corresponds to an uncertainty of about 1 Å in the optical measurement of the red shift.

(b) *Correction for Beam Broadening*

The observed rotation curve has been derived from line profiles, which are the summation of contributions along the line of sight through the galaxy. The observed velocities at the profile peaks will then differ slightly from the actual rotation. The finite bandwidth will also change the shape of the rotation curve. Moreover, important distortion occurs because the size of the galaxy NGC 3109 is comparable with the antenna beam. However, it is possible to make some correction for the effect of the beam, considering that this effect is composed of (i) a shift of the profile peaks along the velocity axis (in combination with the finite bandwidth) and (ii) a broadening of the source.

First, consider the one-dimensional situation of Figure 5, which shows the rotation curve and the distribution of peak brightness temperature $T_{\mathrm{b,max}}$ of the line profiles along the major axis as both would have been observed with an infinitesimally narrow beam. In practice the beam has a finite width, as indicated in Figure 5 where the beam axis is pointing in the direction α. Let PA and BA be the peak brightness temperature and the antenna directivity respectively in the direction A. The antenna temperature will reach its peak value for that frequency for which the product

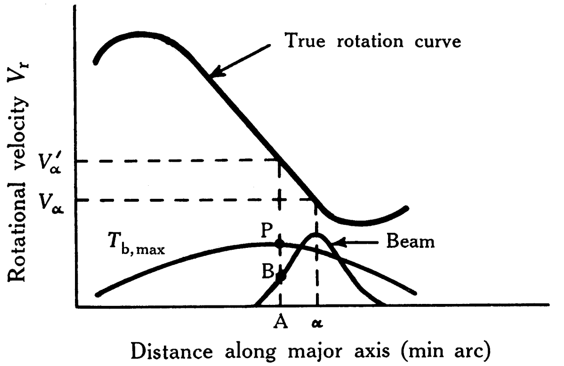

Fig. 5.—Diagram illustrating distortion of the rotation curve by the finite beamwidth (one-dimensional case).

PA $\times$ BA reaches a maximum. When the receiver bandwidth is not very narrow, the product PA $\times$ BA should be averaged over the band. This procedure enables us to construct an observed rotation curve from the "true" curve. Conversely, we can use an analogous process to determine an approximation to the "true" rotation curve, starting from the observed curve and the distribution of the peak antenna temperature.

The restoration process was carried out in two steps:

A. correction for the difference between the observed velocity of the profile peak and the rotational velocity V_α in the direction α, following the procedure outlined above;

B. correction for source broadening by the beam; this was required because the curve of peak antenna temperature, instead of brightness temperature, was used in *A*.

Corrections *A* and *B* are not independent. The restored rotation curve *AB* obtained by this process differs little from that obtained by applying the corrections in reverse order (*BA*). Both restored curves *AB* and *BA* are shown in Figure 6; the interaction of the two corrections is seen to be not serious. The shape of the tails of the corrected curves is uncertain.

In the case of NGC 3109, a one-dimensional treatment of the observed rotation curve was sufficient. For this edge-on system, the contours of constant velocity were closely parallel to the minor axis, and $T_{a,\max}$ was distributed fairly symmetrically about the major axis. A two-dimensional check yielded negligible difference.

(c) *Estimates of Mass*

The rotation curve AB in Figure 6 has been the starting point for the computation of the total mass of the galaxy. Four different methods were followed (de Vaucouleurs 1959).

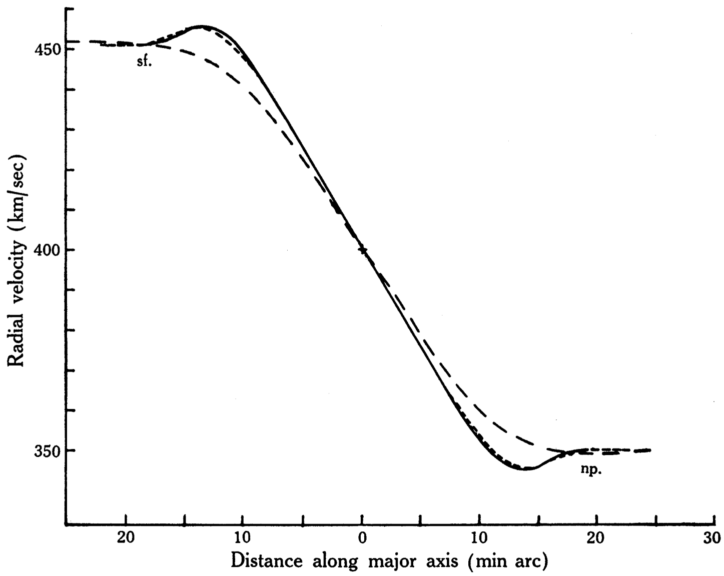

Fig. 6.—Rotation curves for NGC 3109 corrected for beam broadening. – – – observed curve; —— correction AB; - - - - correction BA.

(i) *Keplerian method.*—An estimate of the total mass can be made if we assume that the matter at the border of the galactic plane moves in a circular orbit in the field of a central mass of negligible dimensions. This leads to

$$M_{\mathrm{T}} = \frac{v_{\mathrm{rot}}^2 R}{G}, \tag{8}$$

where G is the gravitational constant and v_{rot} is the rotational velocity at the radius R. For $v_{\mathrm{rot}} = 50 \cdot 9$ km/sec and $R = 22' \cdot 3$ arc $= 14 \cdot 3\, c$ kpc, we have

$$M_{\mathrm{T}} = 0 \cdot 85\, c \times 10^{10} M_{\odot}. \tag{9}$$

(ii) *Lohmann's method.*—Lohmann (1954) describes the force curve in the equatorial plane of a galaxy by an empirical formula due to Bottlinger

$$F = \frac{ar}{1+br^3}; \tag{10}$$

then

$$v^2 = \frac{ar^2}{1+br^3}, \tag{11}$$

where v is the rotational velocity at radius r. If v_{m} and r_{m} are the coordinates of the maximum of the rotation curve, we have

$$a = 3(v_{\mathrm{m}}/r_{\mathrm{m}})^2, \qquad b = 2r_{\mathrm{m}}^{-3}.$$

This leads to

$$M_{\mathrm{T}} = \frac{a}{bG} = \frac{3}{2}\frac{v_{\mathrm{m}}^2 r_{\mathrm{m}}}{G} \tag{12}$$

as long as (10) describes the force field correctly. Figure 7(i) shows that the theoretical rotation curve does not fit rotation curve *AB* very well. For $v_{\mathrm{m}} = 55\cdot5$ km/sec and $r_{\mathrm{m}} = 13'\cdot8$ arc $= 8\cdot8\,c$ kpc, we find

$$M_{\mathrm{T}} = 0\cdot94\,c\times10^{10}\,M_{\odot}, \tag{13}$$

which value is probably too high, since the theoretical rotation curve starts too steeply.

(iii) *Perek's method* (*oblate spheroid*).—Perek (1950, 1962) describes the mass distribution in an oblate spheroid

$$\frac{x^2+y^2}{a^2}+\frac{z^2}{c^2} = m^2$$

by

$$\rho = \rho_{\mathrm{c}}(1-m^2)^n \qquad 0 \leqslant m \leqslant 1, \tag{14}$$

where ρ_{c} is the central density and n a parameter. For the axis ratio c/a, we adopted the value $0\cdot14$ based on optical data (Epstein 1962). Defining $\cos\psi_0 = c/a$, this leads to $\psi_0 = 1\cdot43$ rad. The force curve corresponding to rotation curve *AB* was computed. Entering Perek's tables with the chosen value of ψ_0 to calculate his theoretical force curve, a least-squares solution of ρ_{c} for the case $n = 2$ was obtained:

$$\rho_{\mathrm{c}} = 0\cdot96\;c^{-2}\times10^{-24}\;\mathrm{gm/cm^3}. \tag{15}$$

The theoretical rotation curve is plotted in Figure 7(i). Calculations were made for the case $n = 1$ as well, but these resulted in a badly fitting curve (Fig. 7(i)).

The projected central density for $n = 2$ is

$$\sigma_{\mathrm{c}} = 6\cdot3\,c^{-1}\times10^{-3}\;\mathrm{gm/cm^2}, \tag{16}$$

and the projected density distribution is as shown in Figure 8. Calculation of the total mass yields

$$M_{\mathrm{T}} = 0\cdot56\,c\times10^{10}\,M_{\odot}. \tag{17}$$

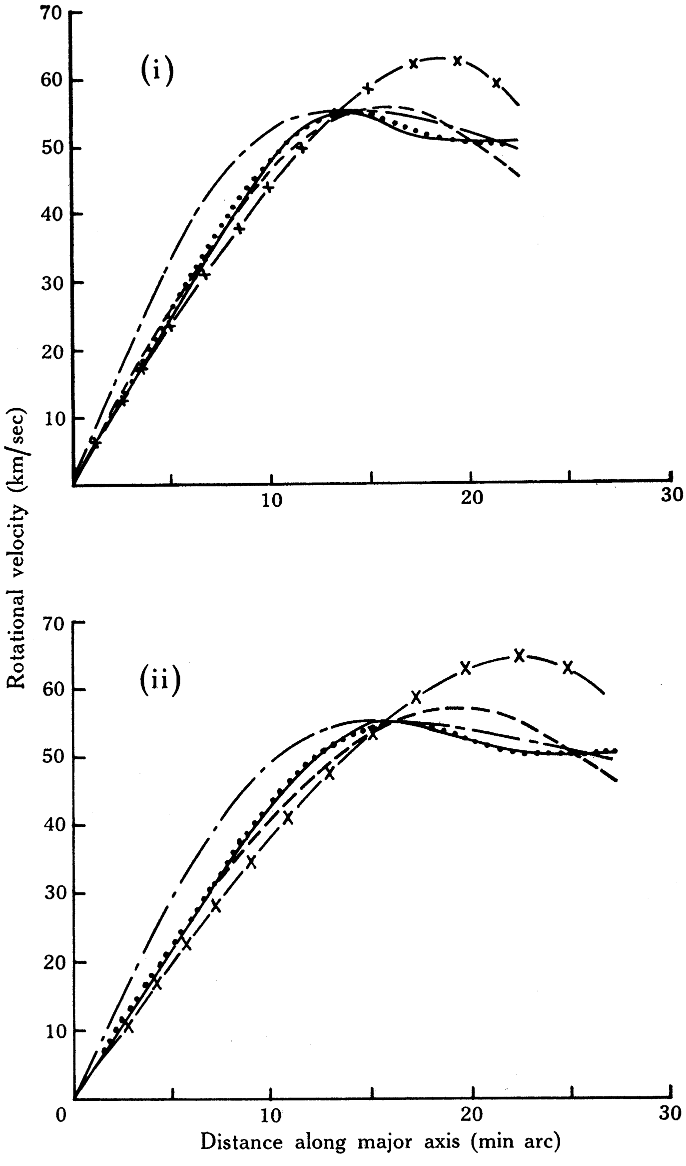

Fig. 7.—Model rotation curves for NGC 3109. (i) Restored rotation curve AB; (ii) restored rotation curve A. —— restored curve; — - — Lohmann function; ····· Wyse and Mayall model; $-\times-\times-$ Perek oblate spheroid ($n = 1$); - - - - Perek oblate spheroid ($n = 2$).

(iv) *Method of Wyse and Mayall (thin disk model)*.—The power series approximation (Wyse and Mayall 1942) for the projected density is

$$\sigma = A+B\alpha+C\alpha^2+D\alpha^3+E\alpha^4+F\alpha^5 \qquad \alpha = r/R \leqslant 1\,, \tag{18}$$

with

$$A+B+C+D+E+F = 0\,,$$

where R is the radius of the galaxy in the principal plane. A least-squares solution for B, C, D, E, F to fit the force curve related to the rotation curve AB was computed using the SILLIAC electronic computer. The values are

B: $+78\cdot1302586$	E: $-2845\cdot9777978$
C: $-566\cdot3104136$	F: $+1160\cdot6909068$
D: $+2247\cdot0972816$	A: $-73\cdot6302356$.

The corresponding theoretical curve is shown in Figure 7(i) and coincides well with curve AB.

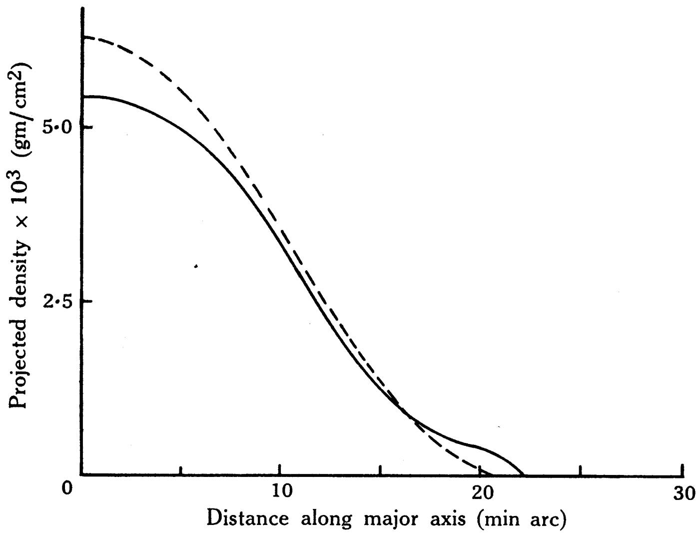

Fig. 8.—Projected density distributions for Wyse and Mayall model (——) and for Perek oblate spheroid with $n = 2$ (– – – –).

Calculation of the projected central density gives

$$\sigma_{\mathrm{c}} = 5\cdot6\,c^{-1}\times10^{-3}\ \mathrm{gm/cm^2}\,, \tag{19}$$

in good agreement with (16). The projected density distribution is shown in Figure 8. The total mass is

$$M_{\mathrm{T}} = 0\cdot53\,c\times10^{10}\,M_{\odot}\,. \tag{20}$$

(d) *Discussion of Results for Total Mass*

The Keplerian result $M_{\mathrm{T}} = 0\cdot85\,c\times10^{10}\,M_{\odot}$ should provide a lower limit to the total mass. Lohmann's result $M_{\mathrm{T}} = 0\cdot94\,c\times10^{10}\,M_{\odot}$ (equation (13)) is probably too high, since the theoretical rotation curve is too steep (Fig. 7(i)). It does not seem unreasonable to set an upper limit of $M_T \leqslant 0 \cdot 9\, c \times 10^{10}\, M_\odot$. Perek's result $M_T = 0 \cdot 56\, c \times 10^{10}\, M_\odot$ ((17) above) is related to a theoretical rotation curve, which closely approximates to curve AB. The assumed axis ratio $c/a = 0 \cdot 14$ is uncertain. Moreover, Perek's method has a tendency to neglect the outer regions of the galaxy, causing the value (17) to be too small. The same holds for the value $M_T = 0 \cdot 53\, c \times 10^{10}\, M_\odot$ of Wyse and Mayall (20) based on a theoretical curve which again fits curve AB very well. The thin disk approximation, however, describes the physical situation less well than Perek's model, yet both results for M_T are in good agreement. As a check, we computed for both methods the projected density distributions (Fig. 8). Here, too, both methods support each other. As a final value for the total mass of NGC 3109, we shall adopt the value

$$M_T = 0 \cdot 6\, c \times 10^{10}\, M_\odot. \tag{21}$$

The uncertainties in the orientation of the system have only a slight influence on the computed mass. It has been assumed that the galaxy is edge-on; a tilt of up to 15° would increase the value of M_T by about 10%. The rotation curve used is that for the optical major axis; it can be seen from the profiles in Figure 2 that the rotation curve would not change significantly if the radio major axis (Section V(b)) were used.

The process of de-smoothing the rotation curve modifies the estimate of M_T. The greatest uncertainty is in correction B of Section VI(b), where a Gaussian HI distribution was assumed. For other HI distributions, the mass would not be changed by more than 20%. This can be shown by computing the mass for the rotation curve in Figure 7(ii), to which only correction A has been applied. The results for the different models are

(i) Keplerian method : $M_T = 1 \cdot 04 \times 10^{10}\, M_\odot$;

(ii) Lohmann method : $M_T = 1 \cdot 10 \times 10^{10}\, M_\odot$;

(iii) Perek method : $M_T = 0 \cdot 70 \times 10^{10}\, M_\odot$;

(iv) Wyse and Mayall method : $M_T = 0 \cdot 65 \times 10^{10}\, M_\odot$.

It can be seen that the adopted mass of $0 \cdot 6 \times 10^{10}\, M_\odot$ is probably somewhat low, but M_T is unlikely to exceed $0 \cdot 9 \times 10^{10}\, M_\odot$.

VII. Conclusions

The atomic hydrogen content of NGC 3109 was found to be

$$M_H = 2 \cdot 2(\pm 0 \cdot 2)c^2 \times 10^9\, M_\odot$$

(corrected for self-absorption) and the total mass of the galaxy $M_T = 0 \cdot 6\, c \times 10^{10}\, M_\odot$, based on a distance $d = 2 \cdot 2\, c$ Mpc. The estimate of the total mass is probably somewhat too small, but M_T is unlikely to exceed $0 \cdot 9\, c \times 10^{10}\, M_\odot$.

To conclude, we give in Table 2 a comparison with results obtained by Epstein (1964). We have used the same correction for self absorption, putting $F = 1\cdot32$ ($F = \overline{C}$ in Epstein's notation). The distance of NGC 3109 is taken to be $2\cdot2$ Mpc.

TABLE 2

SUMMARY OF RESULTS FOR NGC 3109

	L_{pg} ($10^{10}\,L_\odot$)	M_T ($10^{10}\,M_\odot$)	M_H/F ($10^9\,M_\odot$)	M_H ($10^9\,M_\odot$)	M_H/M_T	M_T/L_{pg}	M_H/L_{pg}
Present paper	0·08	0·6	1·7	2·2	0·36	7·5	2·8
Epstein (1964)	0·08	0·69	1·4	1·9	0·28	9	2·5

VIII. Acknowledgments

I wish to thank Dr. B. J. Robinson for many interesting and instructive discussions and Dr. N. U. Mayall for clarification of a mathematical problem. I am much obliged to Mr. J. A. Koehler for his contribution to this investigation, and I thank Miss G. D. Castleman for her assistance with the SILLIAC computer. Dr. Curt Roslund kindly made available the photograph of the galaxy.

IX. References

Bečkvář, A. (1959).—"Atlas Coeli II, Katlog 1950·0." (Nakladatelství, Československé Academie Praha.)

Boss, B. (1963).—General Catalogue. *Publs Carnegie Instn* No. 468.

Bowen, E. G., and Minnett, H. C. (1962).—*J. Br. Instn Radio Engrs* **23**, 49.

Dieter, N. H. (1962).—*Astr. J.* **67**, 217.

Epstein, E. E. (1962).—Thesis, Harvard University.

Epstein, E. E. (1964).—*Astr. J.* **69**, 490.

Howard, W. E. (1961).—*Astr. J.* **66**, 521.

van de Hulst, H. C., Muller, C. A., and Oort, J. H. (1954).—*Bull. astr. Insts Neth.* **12**, 117.

Humason, M. L., Mayall, N. U., and Sandage, A. R. (1956).—*Astr. J.* **61**, 97.

Lohmann, W. (1954).—*Z. Astrophys.* **35**, 159.

National Geographic Society (1954–58).—"Palomar Observatory Sky Atlas."

Perek, L. (1950).—*Bull. astr. Insts Csl.* **2**, 75.

Perek, L. (1962).—*Adv. Astr. & Astrophys.* **1**, 165.

Robinson, B. J. (1963).—*Proc. Instn Radio Engrs Aust.* **24**, 119.

Robinson, B. J., and van Damme, K. J. (1966).—*Aust. J. Phys.* **19**, 111.

Seeger, Ch. L., Westerhout, G., and van de Hulst, H. C. (1956).—*Bull. astr. Insts Neth.* **13**, 81.

de Vaucouleurs, G. (1959).—*In* "Handbuch der Physik". Vol. 53, p. 348. (Springer-Verlag: Berlin.)

Volders, L. (1959).—*Bull. astr. Insts Neth.* **14**, 323.

Wyse, A. B., and Mayall, N. U. (1942).—*Astrophys. J.* **95**, 24.

Appendix I

Calculation of Mass of Neutral Hydrogen

Consider the one-dimensional peak function (point source)

$$\left.\begin{aligned} T_{\mathrm{b}}(x) &= T_{\mathrm{b}0} && x_0 \leqslant x \leqslant x_0+\Delta x, \\ &= 0 && x < x_0,\ x > x_0+\Delta x, \end{aligned}\right\} \tag{A1}$$

and the one-dimensional kernel (beam function)

$$\left.\begin{aligned} h(\xi) &> 0 && -a \leqslant \xi \leqslant +a, \\ &= 0 && \xi < -a,\ \xi > +a, \end{aligned}\right\} \tag{A2}$$

with

$$N \int_{-a}^{+a} h(\xi)\,\mathrm{d}\xi = 1\,. \tag{A3}$$

Scanning $h(\xi)$ over $T_{\mathrm{b}}(x)$, we obtain the equality

$$T_{\mathrm{b}0}\,\Delta x = \int_{x_0}^{x_0+\Delta x} T_{\mathrm{b}}(x)\,\mathrm{d}x = \int_{\mathrm{D}} T_{\mathrm{a}}(x)\,\mathrm{d}x\,, \tag{A4}$$

where D is the convolved integration interval Δx and

$$T_{\mathrm{a}}(x) = N \int_{-a}^{+a} T_{\mathrm{b}}(x-\xi)\,h(\xi)\,\mathrm{d}\xi\,. \tag{A5}$$

This result is independent of the shape of the antenna beam.

Equation (A5) neglects the antenna stray factor β (Seeger, Westerhout, and van de Hulst 1956). We should therefore write

$$T_{\mathrm{a}}(x) = N(1-\beta) \int_{\mathrm{beam}} T_{\mathrm{b}}(x-\xi)\,h(\xi)\,\mathrm{d}\xi\,. \tag{A6}$$

We know (van de Hulst, Muller, and Oort 1954; Volders 1959) that the neutral hydrogen content is given by

$$M_{\mathrm{H}}/M_{\odot} = 3\cdot 10\times 10^{-6} F c^2 d^2 \iiint_{\mathrm{G},\nu} T_{\mathrm{b}}(\theta,\phi,\nu)\,\mathrm{d}\Omega\,\mathrm{d}\nu\,. \tag{2}$$

The galaxy can be considered as a set of point sources. Using (A4) and (A6) for the analogous three-dimensional case in the limit as $\Delta \to d$, equation (2) transforms to

$$M_{\mathrm{H}}/M_{\odot} = 3\cdot 10\times 10^{-6} F c^2 d^2 \iiint_{\mathrm{D},\nu} \frac{T_{\mathrm{a}}(\theta,\phi,\nu)}{1-\beta}\,\mathrm{d}\Omega\,\mathrm{d}\nu\,, \tag{3}$$

where the meaning of the symbols and their units is as given in the text.

Dieter (1962) gives a formula due to Goldstein, neglecting self-absorption,

$$\iint_{\text{source}} N_{\mathrm{H}}\,\mathrm{d}\theta\,\mathrm{d}\phi = 3\cdot 87\times 10^{14}\left(\frac{r^2\lambda^2}{A_{\mathrm{a}}}\right)\left(\iiint_{\mathrm{C}} T_{\mathrm{a}}\,\mathrm{d}\nu\,\mathrm{d}\theta\,\mathrm{d}\phi\right)\Big/\left(\iint_{\mathrm{S}} f(x,y)\,\mathrm{d}x\,\mathrm{d}y\right) \tag{A7}$$

in CGS units. Since

$$A_{\mathrm{a}}\,\Omega_{\mathrm{B}} = A_{\mathrm{a}}\frac{\Omega'_{\mathrm{B}}}{1-\beta} = \frac{A_{\mathrm{a}}}{1-\beta}\iint_{\mathrm{S}} f(x,y)\,\mathrm{d}x\,\mathrm{d}y = \lambda^2$$

(Seeger, Westerhout, and van de Hulst 1956), formulae (A7) and (3) agree.

Appendix II

Source Broadening by Antenna Beam

To calculate a correction for the source broadening, we make use of the fact that the galaxy is seen nearly side-on and approach the problem as a one-dimensional one. Let the antenna beam be represented by the Gaussian function $h(x) = \exp(-mx^2)$. Assume, further, a Gaussian distribution of neutral hydrogen

$$H(x) = \int_{\nu} T_{\mathrm{b}}(x,\nu)\,\mathrm{d}\nu = C\exp(-ax^2)\,. \tag{A8}$$

The convolved HI distribution is

$$\begin{aligned}\tilde{H}(\alpha) &= \int_{\nu}\mathrm{d}\nu\int_{-\infty}^{+\infty} T_{\mathrm{b}}(\alpha-x,\nu)\,h(x)\,\mathrm{d}x\\ &= \int_{-\infty}^{+\infty} H(\alpha-x)\,h(x)\,\mathrm{d}x\,.\end{aligned} \tag{A9}$$

Substitution of (A8) and $h(x)$ yields

$$\tilde{H}(\alpha) = C\exp\left(-\frac{am\alpha^2}{a+m}\right)\int_{-\infty}^{+\infty}\exp\left\{-(a+m)\left(x-\frac{a\alpha}{a+m}\right)^2\right\}\,\mathrm{d}x\,. \tag{A10}$$

The integral in (A10) is a constant if the skirts of the beam are sufficiently extended. Then,

$$\tilde{H}(\alpha) = A\exp\{-am\alpha^2/(a+m)\}\,. \tag{A11}$$

Let

$$h(x_n) = (1/n)\,h(0)\,, \tag{A12}$$

$$H(s_n) = (1/n)\,H(0)\,, \tag{A13}$$

$$\tilde{H}(\alpha_n) = (1/n)\,\tilde{H}(0)\,. \tag{A14}$$

The solutions are respectively

$$x_n^2 = (1/m)\ln n\,, \tag{A15}$$

$$_n^2 = (1/a)\ln n\,, \tag{A16}$$

$$\alpha_n^2 = \left(\frac{a+m}{am}\right)\ln n\,; \tag{A17}$$

therefore,

$$s_n^2 = \alpha_n^2 - x_n^2\,. \tag{A18}$$

By means of (A12), (A13), (A14), and (A18), the convolved source can be corrected along its major axis (Section VI(b)). The same simple relationships hold for a circular source and beam with Gaussian functions. For NGC 3109, we have also applied the same procedure along the minor axis (Section V(b)).